Synthesis and Crystal Structure of Manganese(II) Complexes with 2-Acetylpyridine Methyldithiocarbazate

Seong-Jong Mo, Woo-Taik Lim†, and Bon-Kweon Koo*

Department of Chemistry, Catholic University of Taegu-Hyosung, Kyungsan 713-702, Korea
†Department of Chemistry, Kyungpook National University, Taegu 702-701, Korea
Received May 13, 1998

The aerobic reaction of 2-(acetylpyridine)-S-methyldithiocarbazate (acpy-mdtcH) and 2-(acetylpyridine)-N-phenylthiosemicarbazate(acpy-phTscH) with manganese(II) acetate affords Mn(acpy-mdtc)2 and Mn(acpy-phTsc)$_2$, respectively. The spectroscopic data and X-ray structure of Mn(acpy-mdtc)$_2$ are reported. Crystal data for Mn(acpy-mdtc)$_2$; $C_{18}H_{20}N_6S_4Mn$, mol wt 503.58, monoclinic crystal system($P2_1/c$) a=12.240(5) Å, b= 10.918(1) Å, c=17.651(3) Å, β=105.93(2), and V=2268(1) Å^3, Z=4, 5071 data collected with $0° < 2\theta < 52.64°$, 2995 data with $I > 3\sigma(I)$, R= 0.046, R_w=0.065. The ligands act as tridentate NNS donors. The two Mn-S distances are not equal, and respectively 2.512(2) Å and 2.541(2) Å. The average Mn-N (azomethine) length, 2.242(5) Å, is slightly shorter than the average Mn-N (pyridyl) length, 2.262(5) Å. The coordination environment about Mn(II) center deviates considerably from octahedral geometry. The manganese(II)-manganese(I) and manganese(I)-manganese(0) reduction potentials of Mn(acpy-mdtc)$_2$ are ~-1.71 and ~-1.98 V while those of Mn(acpy-phTsc)$_2$ are ~-1.87 and ~-2.11 V *vs.* Ag/Ag$^+$ in dimethyl sulfoxide, respectively.

Introduction

Manganese can adopt a wide variety of oxidation states and this ability is certainly related to the redox function of the metal ion in biological systems. It is now firmly established that at least three enzymes such as manganese catalase, ribonucleotide reductase of certain bacteria, and the photosystem II of green plants use manganese in redox roles at their catalytic center to facilitate the metabolism of the O_2^{n-} unit.[1-7] Therefore, many manganese complexes containing biomimetic Schiff base ligands have been characterized as the model compounds. In this context, the motivation of this study is due to the experimental chemotherapeutical importance of α-N-heterocyclic carboxaldehyde thiosemicarbazones and their complexes. It has been known that 2-acetylpyridine thiosemicarbazone(Ia) possesses significant antimalarial[8,9] and antileukemic activity.[10]

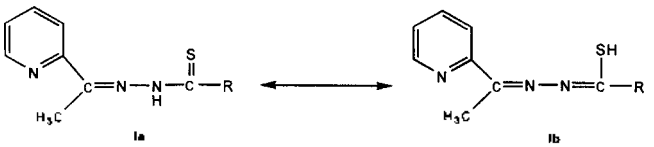

The molecular features that have been shown to be essential for antimalarial activity are the presence of 2-pyridylalkylidene moiety.[9] These features would also be expected to promote effective transition-metal chelating properties.[11]

Saryan *et al.*[12] have shown that the iron complexes of some α-N-heterocyclic thiosemicarbazones are three- to sixfold more active as inhibitors of ribonucleotide reductase than the free ligands. They also noted an intensification of antitumor activity upon complexation.

In view of these considerations, we decided to prepare manganese complexes of 2-acetylpyridine-S-methyldithiocarbazate(acpy-mdtc^{-1}) and 2-acetylpyridine-N-phenylthiosemicarbazate(acpy-phTsc^{-1}) as models for their antimalarial and antitumor properties. We now describe the synthesis, spectroscopic and electrochemical properties, and X-ray crystal structure for these manganese(II) complexes.

Experimental Section

Materials. Solvents and reagents were obtained from commercial sources and used as received. Mn(CH$_3$COO)$_2$·4H$_2$O was purchased from Junsei Chemical Co. 2-Acetylpyridine and 4-phenyl-3-thiosemicarbazide were obtained from Aldrich Chemical Co. All other chemicals and solvents were reagent grade. The ligand [NC$_5$H$_4$CCH$_3$NNHC(S)R] (R= SCH$_3$, NHC$_6$H$_5$) were prepared as described in the literature.[13]

Measurements. Carbon, Hydrogen, Nitrogen, and Sulfur analyses were carried out using a Carlo Erba Model EA-1106 CHNS/O Analyzer. The IR spectra were recorded as KBr disks using a Mattson Polaris FT-IR spectrophotometer in the 4,000-500 cm^{-1} region and UV-Vis spectra were obtained in CH_2Cl_2 or DMF using a Milton Roy Spectronic Genesys 2 spectrophotometer. ^{1}H NMR spectra of CD_2Cl_2 or DMSO-d_6 solutions were obtained on a Varian Gemini-200 spectrometer. Chemical shifts are in ppm relative to internal Me_4Si. Molar conductivities were measured with a YSI Model 31 conductivity bridge. Melting points were carried out with a Laboratory Devices Inc. Mel-Temp II. Electrochemical measurements were performed using a EG&G Model 263 electrochemical system. A three-electrode cell comprising a platinum electrode, a platinum-wire counter electrode, and a Ag/Ag$^+$ was used. The solute concentrations were 1×10^{-3} M with 0.1 M tetraethylammonium perchlorate (supporting elecrolyte) in distilled dimethyl sulfoxide (10 mL).

Bis(2-acetylpyridine-S-methyldithiocarbazate) manganese(II) 1. To a stirred yellow solution of 2-acetylpyridine-S-methyldithiocarbazate (0.45 g, 2 mmol) in methanol (25 mL) was added Mn(O$_2$CCH$_3$)$_2$·4H$_2$O (0.25 g, 1

mmol) at room temperature. The mixture solution was refluxed for one hour. The redish-brown solid was collected by filtration, washed with a little cold methanol and diethyl ether, and dried in vacuum oven (25 mmHg, 25 °C) for one day. Yield: 0.35 g (70%). mp 269 °C. Anal. Calcd for $C_{18}H_{20}N_6S_4Mn$: C, 42.93; H, 4.00; N, 16.69; S, 25.47. Found: C, 42.77; H, 4.00; N, 16.89; S, 25.14. IR (on KBr pellet, cm^{-1}): 2916, 1586, 1553, 1407, 1299, 1138, 1044, 1016, 932, 806, 775, 742, 712, 667, 610.

Bis(2-acetylpyridine-N-phenylthiosemicarbazate) manganese(II) 2. The complex was prepared according to the similar method used for 1, except that acpy-phTscH was used instead of acpy-mdtcH. Yield: 0.43 g(72%). mp 290 °C (dec.). Anal. Calcd for $C_{28}H_{26}N_8S_2Mn$: C, 56.65; H, 4.41; N, 18.88; S, 10.80. Found: C, 56.59; H, 4.40; N, 18.96; S, 10.69. IR (on KBr pellet, cm^{-1}): 2923, 1594, 1540, 1492, 1453, 1415, 1316, 1234, 1179, 1146, 1074, 890, 850, 826, 765, 744, 682, 667, 650, 614.

Crystal Structure Determination of 1. A dark brown crystal of **1**, approximately 0.20×0.20×0.20 mm, was crystallized from CH_2Cl_2/ether (0 °C) and mounted in glass capillary. Measurement was made on a Enraf-Nonius CAD4 TURBO diffracto- meter using Mo-K_α radiation (λ= 0.71069 Å) monochromatized from a graphite crystal whose diffraction vector was parallel to the diffraction vector of the sample and anode generator. Preliminary experiments for the cell parameters and orientation matrix for crystal was carried out by least-squares refinement, using the setting angles of 25 carefully centered reflections in the range $20° < 2\theta < 35°$. Diffraction intensity was collected at a constant temperature of 20(1) °C using the ω-2θ scan technique with variable scan speeds. Omega scans of several intense reflections were made prior to the data collection to optimize the proper scan width for crystal.

The intensities of three representative reflections which were measured after every 150 reflections remained constant throughout data collection indicating crystal and electronic stability for crystals. Of the reflections collected, those with $I > 3\sigma(I)$ were used for structure determination. The structure was solved by direct method (MULTAN)[14] and subsequent Fourier difference technique, and refined anisotropically, by full-matrix least-squares, on F^2 (program MolEN).[15] Hydrogen atoms were included in idealized positions with isotropic thermal parameters riding on those of the parent carbon atoms.

Results and Discussion

Synthesis and Spectral Properties. The reaction of manganese(II) acetate tetrahydrate with either ligand acpy-mdtcH or acpy-phTscH in methanol affords the corresponding redish-brown solids. Elemental analysis and spectral data suggest that the formulations are monomeric [MnL_2]. The manganese complex **1** is readily soluble in common organic solvents, but **2** not soluble except DMF and DMSO. The molar conductivity of **1** and **2** shows small values in CH_2Cl_2 and DMF, respectively (Table 1). These results indicate that the complexes are non-electrolytes.[16] The infrared spectra indicate the mode of the ligand coordination. The peak near 1590 cm^{-1} is assigned to the ring deformation mode. Positive shift of the mode compared to that of the free ligand indicates that the pyridyl nitrogen coordinates to the manganese moiety. The stretching mode ν(CS) near 770 cm^{-1} is significantly decreased. This could involve an azine ↔ imine-hydrazone tautomerism, *i.e.* a 1,3-proton shift. The UV/Vis spectra of these complexes **1, 2** were recorded in the region 200-700 nm and the resultant data were given in Table 1. In the complex **1** the absorption near 400 nm may be assigned to the charge transfer band and that near 330 nm to the $\pi \rightarrow \pi^*$ ligand band comparing to its free ligand (335 nm).

Table 1. Conductivity and UV/Vis Spectral Data for Complexes **1**[a] and **2**[b]

Complex	UV/Vis data	Λ_M
	λ_{max}/nm (logε/dm^3 mol^{-1} cm^{-1})	(Mho cm^2 mol^{-1})
1	329 (4.36)	2.1
	404 (4.34)	
2	277 (4.48)	1.8
	398 (4.58)	

[a] in CH_2Cl_2. [b] in DMF.

Although elemental analysis and all the spectral data of **1, 2** are consistent with the schematic structure shown in eq. 1, it was not possible to deduce the exact structure of the complexes. Hence we undertook a crystallographic investigation to determine the solid state structure.

Table 2. Crystallographic Data and Intensity Collection for complex **1**

Empirical formula	$C_{18}H_{20}N_6S_4Mn$
F_w	503.58
Crystal system	monoclinic
Space group	$P2_1/c$(#14)
Z	4
Cell parameters	
a(Å)	12.240(5)
b(Å)	10.918(1)
c(Å)	17.651(3)
β(°)	105.93(2)
V(Å^3)	2268(1)
D_{calc}(g/cm^3)	1.475
μ (cm^{-1} with Mo-K_α)	13.6
Transmission factor	94.5427-99.9308
Scan type	ω-2θ
Scan width(ω)(deg)	1.09+0.71tan(θ)
$2\theta_{max}$(deg)	52.64
No. of reflections measured	5071
No. of reflections observed ($I > 3\sigma(I)$)	2995
No. of variable	262
Discrepancy indices	
R^a	0.046
R_w^b	0.065
Goodness of fit indicator[c]	1.97
Maximum shift in final cycles	less than 0.01

[a] $R=\Sigma||F_o|-|F_c||/\Sigma|F_o|$. [b] $R_w=[(\Sigma w(|F_o|-|F_c|)^2/\Sigma w(F_o^2)]^{1/2}$, where $w=[\sigma(F^2)]^{-1}$. [c] Estimated standard deviation of an observation of unit weight: $[(\Sigma w(|F_o|-|F_c|)^2/(N_o-N_v)]^{1/2}$, where N_o=Number of observations and N_v= Number of variables.

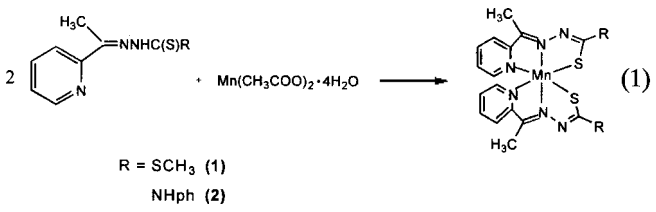

R = SCH_3 (1)
NHph (2)

X-ray Structural Description of 1. A summary of data collection and crystallographic parameters are given in Table 2. Atomic positional parameters are given in Table 3, while selected bond lengths and angles are given in Table 4. The molecular structure and atom-numbering scheme for **1** is shown in Figure 1a. The polyhedral representation of this compound which has been rotated somewhat in order to illustrate the coordination environment, is also shown in Figure 1b. The bond lengths are unremarkable for Mn(II) species.[17] That the manganese ions of both complexes are in oxidation state +2 is confirmed by the ^1H NMR silence due to the paramagnetism of Mn(II) (d^5) and by the bond lengths. The 2-acetylpyridine-S-methyldithiocarbazate ligand acts as tridentate NNS donors. In the molecular structure, the two ligands are approximately equivalent but no crystallographic

Table 3. Fractional Positional Parameters and Displacement Parameters of Non-Hydrogen Atoms with Their Estimated Standard Deviations in Parentheses

Atom	x	y	z	Beq/Å^{2a}
Mn(1)	0.75605(5)	0.08541(7)	0.81056(4)	3.09(1)
S(1)	0.7004(1)	−0.1294(1)	0.83476(8)	3.85(3)
S(2)	0.7447(1)	0.0616(2)	0.66540(8)	4.51(3)
S(3)	0.5233(1)	−0.2196(1)	0.90052(8)	4.55(3)
S(4)	0.9382(1)	−0.0091(2)	0.59995(8)	4.98(3)
N(1)	0.5955(3)	0.1089(3)	0.8473(2)	2.91(8)
N(2)	0.9369(3)	0.0928(4)	0.8064(2)	3.22(8)
N(3)	0.5382(3)	0.0155(4)	0.8722(2)	3.37(8)
N(4)	0.9725(3)	0.0645(4)	0.7400(2)	3.76(9)
N(5)	0.7110(3)	0.2863(4)	0.8059(2)	3.32(8)
N(6)	0.8678(3)	0.1257(4)	0.9334(2)	3.49(9)
C(1)	1.0166(4)	0.1283(5)	0.8658(3)	4.0(1)
C(2)	1.1406(4)	0.1517(7)	0.8685(3)	5.7(2)
C(3)	0.7761(4)	0.3770(5)	0.7901(3)	4.0(1)
C(4)	0.7498(4)	0.4982(5)	0.7923(3)	4.3(1)
C(5)	0.6516(5)	0.5293(5)	0.8095(3)	4.6(1)
C(6)	0.5823(4)	0.4396(5)	0.8255(3)	3.9(1)
C(7)	0.6156(4)	0.3199(4)	0.8241(3)	3.2(1)
C(8)	0.9776(4)	0.1482(5)	0.9411(3)	3.4(1)
C(9)	1.0523(4)	0.1836(5)	1.0115(3)	4.3(1)
C(10)	1.0113(4)	0.1955(5)	1.0756(3)	4.6(1)
C(11)	0.8981(4)	0.1722(6)	1.0694(3)	4.7(1)
C(12)	0.8307(4)	0.1381(6)	0.9965(3)	4.3(1)
C(13)	0.5498(4)	0.2143(5)	0.8472(3)	3.4(1)
C(14)	0.4427(4)	0.2420(5)	0.8687(3)	4.4(1)
C(15)	0.5853(4)	−0.0914(5)	0.8678(3)	3.2(1)
C(16)	0.4046(4)	−0.1547(5)	0.9267(3)	4.8(1)
C(17)	0.8858(4)	0.0441(4)	0.6778(3)	3.5(1)
C(18)	0.8176(6)	−0.0084(7)	0.5156(3)	6.5(2)

[a] Anisotropically refined atoms are given in the form of the isotropic equivalent displacement parameter defined as $4/3[a^2B(1,1)+b^2B(2,2)+c^2B(3,3)+ab(\cos\gamma)B(1,2)+ac(\cos\beta)B(1,3)+bc(\cos\alpha)B(2,3)]$.

Table 4. Selected Bond Distances (Å) and Angles (deg) for complex **1**

Distances

Mn(1)--S(1)	2.512(2)	S(2)--C(17)	1.692(5)
Mn(1)--S(2)	2.541(2)	N(1)--N(3)	1.377(6)
Mn(1)--N(1)	2.246(4)	N(1)--C(13)	1.279(6)
Mn(1)--N(2)	2.237(4)	N(2)--N(4)	1.391(6)
Mn(1)--N(5)	2.257(4)	N(2)--C(1)	1.281(5)
Mn(1)--N(6)	2.266(3)	N(3)--C(15)	1.314(6)
S(1)--C(15)	1.717(5)	N(4)--C(17)	1.320(5)

Angles

S(1)--Mn(1)--S(2)	97.68(5)	C(15)--S(3)--C(16)	102.9(3)
S(1)--Mn(1)--N(1)	76.0(1)	C(17)--S(4)--C(18)	104.7(3)
S(1)--Mn(1)--N(2)	110.9(1)	Mn(1)--N(1)--N(3)	124.8(3)
S(1)--Mn(1)--N(5)	147.0(1)	Mn(1)--N(1)--C(13)	121.3(3)
S(1)--Mn(1)--N(6)	98.0(1)	Mn(1)--N(2)--N(4)	124.2(2)
S(2)--Mn(1)--N(1)	119.50(9)	Mn(1)--N(2)--C(1)	121.4(3)
S(2)--Mn(1)--N(2)	75.6(1)	N(1)--N(3)--C(15)	111.7(4)
S(2)--Mn(1)--N(5)	96.8(1)	N(2)--N(4)--C(17)	111.8(4)
S(2)--Mn(1)--N(6)	146.7(1)	Mn(1)--N(5)--C(7)	118.5(3)
N(1)--Mn(1)--N(2)	163.2(1)	Mn(1)--N(6)--C(8)	117.4(3)
N(1)--Mn(1)--N(5)	71.0(1)	N(2)--C(1)--C(8)	113.7(4)
N(1)--Mn(1)--N(6)	92.7(1)	N(5)--C(7)--C(13)	114.4(4)
N(2)--Mn(1)--N(5)	101.4(1)	N(6)--C(8)--C(1)	115.2(4)
N(2)--Mn(1)--N(6)	71.4(1)	N(1)--C(13)--C(7)	114.7(4)
N(5)--Mn(1)--N(6)	85.6(1)	S(1)--C(15)--N(3)	130.5(4)
Mn(1)--S(1)--C(15)	96.8(2)	S(2)--C(17)--N(4)	130.4(4)
Mn(1)--S(2)--C(17)	96.3(2)		

C_2 axis exists. Due to ligand rigidity, the MnN_4S_2 coordination spheres are subject to very considerable distortions. Thus, the angles at the metal center show large deviations (Table 4) from the ideal octahedral values of 90° and 180°. The molecule contains MnNCCN and MnNNS five membered rings. The Mn(N(5)-N(1)-S(1)) and Mn(N(6)-N(2)-S(2)) fragments constitute a very mediocre plane (mean dviations, 0.02 Å and 0.06 Å, respectively). The pyridylaldimine and azine-thiol rings in either ligand are excellent individual planes (mean deviations, the former fragment; 0.011 Å and 0.035 Å, the latter fragment; 0.070 Å and 0.0047 Å) but there is respectively 3.7° and 7.7° fold at their intersections. In view of above results, overall planarity is relatively superior for the Mn(N(5)-N(1)-S(1)) fragment. The azomethine Mn(1)-N(1) and Mn(1)-N(2) distance in the structure are respectively 2.246(4) Å and 2.237(4) Å, longer than that the Mn(III), Mn(IV) complexes.[18,19] This values are similar to that of typical Mn(II) complexes. The pyridyl Mn (1)-N(5) and Mn(1)-N(6) distances are nearly equal, the average being 2.262(5) Å. This distance is slightly longer than the average distance Mn(1)-N(1) and Mn(1)-N(2) (2.242(5) Å) of azomethine, indicating that the more negatively charged amine atom is a stronger donor to the manganese center than the neutral imine atom. The imine N(3)-C(15) (1.314(6) Å) and N(4)-C(17) (1.320(5) Å) bond distances are shorter than single bond distance of C-N. The short bond distance demonstrates the involvement of the 1,3-proton shift.

Electrochemical Properties. The complexes **1, 2** were electrochemically examined at a platinum working electrode in dimethyl sulfoxide solution. Representative cyclic

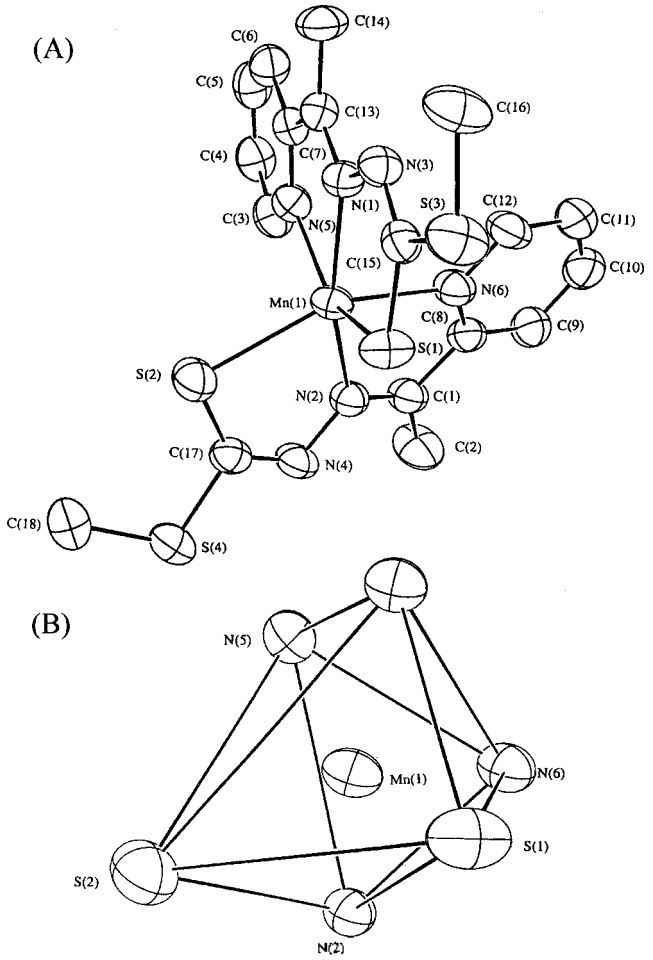

Figure 1. (A) Molecular structure and numbering scheme for complex [Mn(acpy-mdtc)$_2$]. Thermal ellipsoids have been drawn at the 50% probability level. Hydrogen atoms are omitted for clarity. (B) ORTEP plot of the coordination polyhedra about the manganese atom.

Table 5. Reduction Potentials[a] at Room Temperature

compd	Mn(II)-Mn(I) $E_{pc}(E_{pa})^b$, V	Mn(I)-Mn(0) $E_{pc}(E_{pa})^b$, V	scan rate mVs^{-1}
1	−1.70(−1.63)	−1.96(−1.89)	100
2	−1.86(−1.78)	−2.10(−2.00)	100

[a] Supporting electrolyte is TEAP (0.1 M); working electrode is platinum; reference electrode is Ag/Ag^+ (0.01 M). [b] Values in parentheses are coupled oxidation peaks observed with a complete CV cycle.

voltammograms according to the scan rates (50-400 mVs^{-1}) are displayed in Figure 2 and reduction potentials at scan rate 100 mVs^{-1} are listed in Table 5. All potentials are referenced to a Ag/Ag^+ (0.01 M) electrode.

Two cyclic responses for both complexes are observed in the potential range 0.00~−2.20 V. Current height considerations support the same electron stoichiometry for the responses, which is assigned to the electrode $Mn^{II}L_2$-$Mn^{I}L_2^-$ and $Mn^{I}L_2^-$-$Mn^{0}L_2^{2-}$ couples.

In the complex **1** the both couples are quasi-reversible with the peak-to-peak separations (ΔE_p) in the range 70-90 mV regardless of the scan rates. But, in the complex **2** the

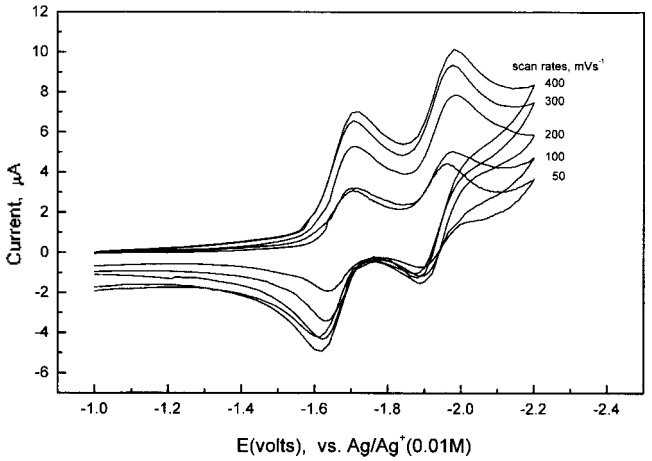

Figure 2. Cyclic voltammogram of ~10^{-3} M solutions (0.1 M TEAP) of [Mn(acpy-mdtc)$_2$] in DMSO.

couples are irreversible and anodic peaks for the reduction responses are absent in 50 mVs^{-1} scan rate. In higher scan rates (100-400 mVs^{-1}), the anodic and cathodic peaks of the manganese(II)-manganese(I) are observable and especially, in above scan rate 200 mVs^{-1}, are quasi-reversible (ΔE_p=70-100 mVs^{-1}). The resulting data suggest that complex **1** is more easily reduced than complex **2** due to the inductive effect of the substituent in dimethyl sulfoxide.

Supporting Information Available. Listing of atomic coordinates, complete bond distances and angles, thermal parameters, and least-squares results for **1** (24 page). Ordering information is given on any current masthead page.

References

1. Beyer, W. F. Jr.; Fridovich, I. *Manganese in Metabolism and Enzyme Function*; Academic Press: New York, 1986; Chapter 12, p 193.
2. Pecoraro, V. L. *Photochem. Photobiol.* **1986**, *48*, 249.
3. Christou, G. *Acc. Chem. Res.* **1989**, *22*, 328.
4. Brudvig, G. W.; Crabtree, R. H. *Prog. Inorg. Chem.* **1989**, *37*, 99.
5. Vincent, J. B.; Christou, G. *Adv. Inorg. Chem.* **1989**, *33*, 197.
6. Wieghardt, K. *Angew. Chem., Int. Ed. Engl.* **1989**, *28*, 1153.
7. Que, L. Jr.; True, A. E. *Prog. Inorg. Chem.* **1990**, *38*, 97.
8. Klayman, D. L.; Bartosevich, J. F.; Griffin, T. S.; Mason, C. J.; Scovill, J. P. *J. Med. Chem.* **1979**, *22*, 855.
9. Klayman, D. L.; Scovill, J. P; Bartosevich, J. F.; Mason, C. J. *J. Med. Chem.* **1979**, *22*, 1367.
10. Scovill, J. P.; Klayman, D. L.; Franchino, C. F. *J. Med. Chem.* **1982**, *25*, 1261.
11. Mathew, M.; Palenik, G. J. *J. Am. Chem. Soc.* **1969**, *91*, 6310.
12. Saryan, L. A.; Ankel, E.; Krishnamurti, C.; Petering, D. H.; Elford, H. *J. Med. Chem.* **1979**, *22*, 1218.
13. Das, M.; Livingstone, S. E. *Inorg. Chim. Acta* **1976**, *19*, 5.
14. Main, P.; Fiske, S. J.; Hull, S. E.; Lessinger, L.; Germain, G.; Declerg, J. P.; Woolfson, M. M. MULTAN 80, University of York, 1980.

15. MolEN, An Interactive Structure Solution Procedure, Enraf-Nonius, Delft, Netherlands, 1990.
16. Geary, W. J. *Coord. Chem. Rev.* **1971**, *7*, 81.
17. Jeffery, J. C.; Thornton, P.; Ward, M. D. *Inorg. Chem.* **1994**, *33*, 3612.
18. Bonadies, J. A.; Kirk, M. L.; Lah, M. S.; Kessissoglou, D. P.; Hatfield, W. E.; Pecoraro, V. L. *Inorg. Chem.* **1989**, *28*, 2037.
19. Dutta, S.; Basu, P.; Chakravorty, A. *Inorg. Chem.* **1991**, *30*, 4031.

Photoresponsive Liquid Crystalline Copolymers Bearing a *p*-Methoxyazobenzene Moiety

Dong Hoon Choi, Suk Hoon Kang, Joon Youl Lee, and Asit Baran Samui*

Division of Textile, Chemical, and Industrial Engineering, Institute of Material Science and Technology, Kyung Hee University, Yongin-shi, Kyungki-do 449-701, Korea
**Naval Materials Research Laboratory, Naval Dockyard, Mumbai 400023, India*
Received May 15, 1998

Mesogenic and azo monomers were synthesized and copolymerized to obtain two copolymers composed of methacrylate and itaconate backbone. Glass transition temperatures of the copolymers were found to be slightly higher than ambient temperature. Both the copolymers showed liquid crystalline properties. *Trans-cis* isomerization in film state was observed under UV-irradiation with a light of 365 nm. Regarding the photochemical phase transition behavior, the transition rate of nematic-to-isotropic state was slightly faster in the methacrylate copolymer during irradiation at 365 nm and the rate of the reverse transition was much faster in itaconate copolymer under thermal effect.

Introduction

There is a considerable interest in the synthesis and characterization of azobenzene containing polymers for several reasons. These materials are found to possess unique optical properties.[1-7] In addition to the studies in the direction of nonlinear optical properties, there is constantly increasing attention in the field of optical data storage and holographic applications. Ikeda et. al. extensively studied the photochemically induced phase transition in polymer liquid crystals containing azobenzene.[8-12] Both azo homopolymers and azo-liquid crystalline (LC) copolymers have been found to be effective media for optical information storage. The mechanism of writing involves photoinduced excitation of the azobenzene group, which undergoes *trans-cis* isomerization. In the case of homopolymers, some extent of *cis* form remains even after thermal treatment. These molecules do not take part in further photochemical excitation and this is translated into birefringence.[13] In the case of azo-LC copolymers the process is different. Rod-like *trans* isomer fits into the LC environment whereas *cis* isomer disturbs it. On UV irradiation the *trans* form isomerizes to the *cis* form. This incident affects the LC environment, inducing a phase transition. LC phase is converted to an isotropic phase. This phenomenon can be used in a photo-recording system.[7]

Few reports appeared in the literature on azo-LC copolymer containing methoxy terminal unit with both comonomers. LC monomers containing the methoxy terminal unit mostly exhibit nematic texture. It was reported that photochemical phase transition is induced more easily in the least ordered nematic LC part compared to other textures of higher order.[10] Itaconate polymers, containing two azobenzene groups per monomer unit, have been found to possess enhanced nonlinear optical properties.[14] It was observed that there was a strong dipole interaction in the LC-itaconate azo copolymer system containing nitro terminal unit with azo part.[15] Similar copolymer having methoxy terminal group is expected to have much less dipole interaction. It seems, therefore, that it will be interesting to study the photochemical phase transition behavior of LC-itaconate azo copolymer containing methoxy terminal groups.

In the present study, we report the synthesis, characterization, *trans-cis* isomerization, photochemical phase transition behavior of methacrylate and itaconate copolymers with LC unit.

Experimental

Synthesis of monomers

4-methoxyphenyl-4'-methacryloyloxy hexyloxy benzoate (MMHB) (M-I). It was synthesized by following the method of Horvath *et al.*[16] using 4-hydroxy benzoic acid as the starting material.

^{1}H NMR (200 MHz, DMSO-d_6): δ (ppm) 8.01 (d, 2H, aromatic), 6.9-7.1 (m, 6H, aromatic), 5.99 (s, 1H, in $C\underline{H}_2$=), 5.63 (s, 1H, in $C\underline{H}_2$=), 4.08 (d, 4H, 2(O-$C\underline{H}_2$)), 3.74 (s, 3H, Ar-O$C\underline{H}_3$), 1.85 (s, 3H, αC-$C\underline{H}_3$), 1.39-1.72 (m, 8H, in -($C\underline{H}_2$)$_4$-).

4-methoxyphenyl methacryloyloxy hexyloxy azobenzene (MMHA) (M-II). 4-methoxy aniline was diazotized by standard technique and reacted with phenol at